Proc. of the Intl. Conf. on Advances In Civil, Structural And Mechanical Engineering- CSM 2014.

ISBN: 978-1-63248-012-5 doi: 10.15224/ 978-1-63248-012-5-79

NUMERICAL INVESTIGATION OF CONVECTIVE HEAT TRANSFER FROM PERFORATED PIN-FINS

[Bayram Şahin, Eyüphan Manay, Kadir Geliş, Süleyman Karslı]

Abstract— In this study, turbulent convection heat transfer and pressure drop from a surface equipped with perforated fins with square cross section were investigated numerically. At constant clearance ratio (C/H=0), the pin-fin spacing ratio in stream wise direction (Sy/D=1.208, 1.944 and 3.4) and the Reynolds number (Re=13.500, 27.500 and 42.000) on heat transfer and pressure drop were examined. RNG based k-ε turbulent model and SIMPLE algorithm were used for governing equations. A constant heat flux of 3200 W/m^2 was applied to the base of pin-fins. The results of the heat transfer and pressure drop characteristics with respect to appropriate variables were presented. The heat transfer increased with increasing Reynolds number and with decreasing clearance ratio and spacing ratio. The fin height of H=100 mm, the spacing ratio of S_y/D=1.208 and the Reynolds number of Re=42.000 were better for cooling processes. The best overall heat transfer enhancement was obtained in the case of S_y/D=1.208, C/H=0 and Re=13.500.

Keywords— *Perforated pin-fin, convective heat transfer, pressure drop, heat transfer enhancement, numerical analysis*

1.INTRODUCTION

The base of heat transfer augmentation process using passive methods is to modify heat transfer surface area. Heat transfer surface area modifications are achieved by mainly adding fins, wings or winglets to the surface. Making these modifications will highly increase heat transfer and pressure drop as expected in comparison with smooth channel, and thus, the parameters effective on heat transfer and pressure drop will be different than that of a smooth channel. The most important ones of these parameters are fin number and geometry, temperature gradient on finned surface and fins, the velocity of the fluid encircling the fins and the thermal conductivity of the material from which fins are constructed [1].

Eyüphan Manay, Bayram Şahin
Erzurum Technical University, Mechanical Engineering Dep.
Erzurum/ Turkey

Veysel Özceyhan
Erciyes University, Mechanical Engineering Dep.
Kayseri/Turkey

Kadir Geliş
Ağrı İbrahim Çeçen University, Mechanical and Metal Tech.
Ağrı/Turkey

As known, enhancing heat transfer surface area enhances heat transfer, nonetheless this increase in surface area leads the pressure drop to increase [2]. Heat transfer from a single fin will be higher than that of a smooth channel; likewise heat transfer from an array of fins will be much higher than single one [3, 4]. Yu et al. [5-7] investigated heat transfer characteristics of a heat sink in the form of plate fin and plate pin fin. The thermal performance of the plate pin fin was better than the plate fin because of lower thermal resistance of the plate pin fin heat sinks. Rounding the fins may lead to lower friction factors and higher thermal performance than rectangular cross-sectioned fins with respect to heating and cooling [8].

In experimental studies, defining the temperature gradient on each fin is highly time consuming and requires great sensitivity. In addition to this, the production of the fins in a sensitive way will bring an additional cost. Because of these difficulties, the investigation of heat and flow characteristics around the fins exposed to the fluid flow inside the channel makes numerical solutions inevitable. Peng and Ling [9] defined heat transfer and flow characteristics of the fins placed into the channel by 3D numerical study. It was observed that heat transfer increased near the channel inlet and decreased towards the end of the channel. Şahin et al. [10] investigated numerically fin-tube type heat exchanger. Heat transfer around the semi spherical holes created at the inner surfaces of the fins was studied numerically by Xien and Sunden [11]. It was found that the perforations on the fins were an effected way of enhancing heat transfer.

The effects of the form of the fins on heat transfer and pressure drop characteristics were investigated by Sahiti et al. [12]. NACA, dropform, lancet, elliptic, circular and square cross sectioned fins were examined in staggered and inline arrangements. It was reported that elliptic fins provided highest heat transfer for a given base area and the same energy input. Li et al. [13] investigated the heat transfer and pressure drop characteristics of an elliptic fin. It was found that the elliptic fin provided higher heat transfer than circular fins. An unsteady heat transfer and flow characteristics around rectangular fins placed into two parallel plates were studied by Saha and Acharya [14]. Heat transfer characteristics of pin fins placed into the trapezoidal ducts were investigated by Hwang and Lui [15, 16].

Perforating the fins will provide extra enhancement to heat transfer. Via the aid of the perforations, the fluid will pass from the inside of the fins, and in this way an extra heat transfer will be provided [17, 18]. In the studies conducted by the perforated fins, perforation diameter and the number of the perforations are the possible alternatives to enhance heat transfer. It was observed that heat transfer increases by the increase of the perforation diameter and the number of the

Proc. of the Intl. Conf. on Advances In Civil, Structural And Mechanical Engineering- CSM 2014.

ISBN: 978-1-63248-012-5 doi: 10.15224/ 978-1-63248-012-5-79

perforations, but the increase of the perforation diameter was more effective than that of the perforation number [19].
The aim of this study is to numerically determine the heat transfer and the pressure drop characteristics of the perforated fins with rectangular cross section under the conditions of different flow velocities and pin-fin spacing ratios. For validation of the numerical method, the results of this study were compared with those in the experimental studies available in literature. For the comparison of the numerical results with the experimental ones, the study of Sahin and Demir [17] was used.

2. NUMERICAL SOLUTION PROCEDURE

2.1. Numerical Modeling

The physical model of the fins has a square cross section of 15 mm x 15 mm, and, the fins were attached on the upper surface of the base plate, as shown in Fig. 1. Square pin fins with for constant C/H value of 0 were perforated at the 17 mm from the bottom tip by an 8 mm diameter. The pin fins were fixed uniformly on the base plate with a constant spacing of 18.125 mm in the spanwise direction, with different spacings in the streamwise direction. The spacing ratios of the pin fins in the streamwise direction (S_y/D) were 1.208, 1.944 and 3.417 mm, giving different numbers of the pin fins on the base plate. It is well known that if the inter-fin spacing in the spanwise direction decreases, the flow blockage will increase and thus, pressure drop along to tested heat exchanger will increase. Because the aim of the study is to determine inter-fin spacing in streamwise direction, the spacings in the spanwise direction were not considered in this study. The Reynolds number range used in this numerical study was 13.500–42.000, which was based on the hydraulic diameter of the channel over the test section (D_h) and the average velocity (u_m). The base plate of the pin fins has a cross section of 250 mm length and 250 mm width.

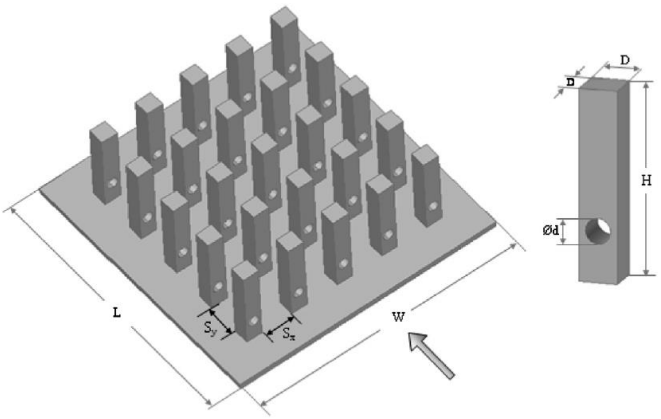

Figure 1. Perspective view of the heat exchanger and a single perforated pin-fin configuration.

2.2. Governing Equations

In all numerical studies, the first step is to determine the equations to simulate the problem. For a given thermo-fluid problem, the related equations are continuity, momentum and energy equations. In this study, the computations are conducted under three dimensional, time independent (steady-state) and turbulent flow conditions. The continuity, momentum and energy equations are given follows:
Contiunity Equation:

$$\frac{\partial u}{\partial x}+\frac{\partial v}{\partial y}+\frac{\partial w}{\partial z}=0 \quad (1)$$

Momentum Equations:

$$V\nabla V=-\frac{1}{\rho}\nabla P+\nu\nabla^2 V \quad (2)$$

Energy Equation:

$$u\frac{\partial T}{\partial x}+v\frac{\partial T}{\partial y}+w\frac{\partial T}{\partial z}=\alpha\left(\frac{\partial^2 T}{\partial x^2}+\frac{\partial^2 T}{\partial y^2}+\frac{\partial^2 T}{\partial z^2}\right) \quad (3)$$

In EqS. 1 and 2, ν is the kinematic viscosity, P is the pressure, T is the temperature, ρ is the density of air. u, v and w are the velocity components in the direction of x, y and z in Cartesian coordinate system, respectively. The above thermo-physical properties of air are taken as temperature independent (constant) properties. Because of the fact that the flow is fully turbulent and molecular viscosity effects are neglected, the turbulent kinetic energy and the dissipation rate of turbulent kinetic energy equations derived from the transport equations are given as below [20]:

$$\nabla(\rho kU)=\nabla\left(\alpha_k\mu_{eff}\nabla k\right)+G_k+G_b-\rho\varepsilon-Y_M+S_k \quad (4)$$

$$\nabla(\rho\varepsilon U)=\nabla\left(\alpha_\varepsilon\mu_{eff}\nabla\varepsilon\right)+C_{1\varepsilon}\frac{\varepsilon}{k}(G_k+C_{3\varepsilon}G_b)-C_{2\varepsilon}\rho\frac{\varepsilon^2}{k}-R_\varepsilon+S_\varepsilon \quad (5)$$

In Eq. 4, Y_M is the contribution of fluctuating dilatation to all diffusion ratios at compressible turbulent. In Eq. 5, $C_{1\varepsilon}$, $C_{2\varepsilon}$ and $C_{3\varepsilon}$ are the model constants, α_k and α_ε are the inverse effective Prandtl number for k and ε. S_k and S_ε are the user defined source terms. Turbulent kinetic energy production (G_k) caused by mean velocity gradient is given by [21]:

$$G_k=-\rho\overline{u'v'}\frac{\partial v}{\partial x} \quad (6)$$

and the turbulent kinetic energy production (G_b) caused by lifting forces is given as follows:

$$G_b=\beta g_x\frac{\mu_t}{\mathrm{Pr}_t}\frac{\partial T}{\partial x} \quad (7)$$

In Eq. 7, Pr_t denotes the turbulent Prandtl number, and g is the gravitational acceleration. Thermal expansion coefficient (β) is defined as:

$$\beta=-\frac{1}{\rho}\left(\frac{\partial\rho}{\partial T}\right)_P \quad (8)$$

In Eq. 4, the term Y_M is calculated by:

Proc. of the Intl. Conf. on Advances In Civil, Structural And Mechanical Engineering- CSM 2014.

ISBN: 978-1-63248-012-5 doi: 10.15224/ 978-1-63248-012-5-79

$$Y_M = 2\rho\varepsilon M_t^2 \qquad (9)$$

Here, M_t is the turbulent Mach number and is given by:

$$M_t = \sqrt{\frac{k}{a^2}} \qquad (10)$$

where a is the speed of sound, and can be written as:

$$a = \sqrt{\gamma RT} \qquad (11)$$

where γ is the specific weight, and R is the gas constant. The turbulent viscosity is

$$\mu_t = \rho C_\mu \frac{k^2}{\varepsilon} \qquad (12)$$

2.3. Computational Domain and Boundary Conditions

In Figure 2, the computational domain which represents a channel with an internal cross-section of 250 mm width and 100 mm height (channel aspect ratio=2.5:1 and hydraulic diameter, D_h=0.143 m) and the boundary conditions applied are presented. The total length of the channel is 3140 mm. As shown in Figure 2, the computational domain mainly consists of the perforated fins (solid), the base plate (solid) and the air surrounding the fins (fluid). Symmetry boundary condition is applied to the left and the right side of the computational domain. At the inlet section, the air is assumed to have uniform velocity and temperature (300 K).

T (K)	ρ (kg/m^3)	c_p (kj/kg K)	μ x 10^7 (Ns/m^2)	ν x 10^6 (m^2/s)	k x 10^3 (W/mK)	α x 10^6 (m^2/s)
300	1.1614	1.007	184.6	15.89	26.3	22.5

Table 1. The thermo-physical properties of air at 300 K.

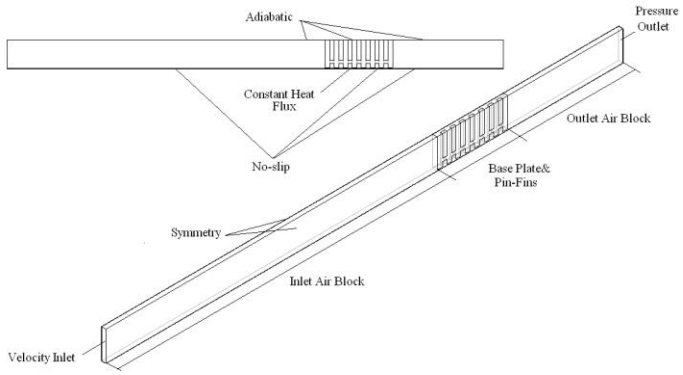

Figure 2. Computational domain and boundary conditions.

The thermo-physical properties of the air at 300 K are presented in Table 1. At the outlet section, pressure outlet boundary condition is applied. The whole upper side of the domain is taken as adiabatic. No-slip boundary condition and a constant heat flux of 3.2 kW/m^2 are applied to the bottom side of the base plate. An eddy diffusivity approximation for the turbulent heat flux is used to predict temperature field.

2.4. Numerical Mesh and Grid Independence

The computational fluid dynamics (CFD) calculations are made by using commercial code of FLUENT version 6.1.22. In all the numerical calculations, segregated manner is selected as solver type due to its advantage which helps preventing from convergence problems and oscillations in pressure and velocity fields of strong coupling between the velocity and pressure. An RNG based k-ε turbulence model is used for simulations. The first order upwind numerical scheme and SIMPLE algorithm are used to discretize the governing equations because they are more stable and economical in comparison with the other algorithms utilized. The converging criterions are taken as 10e-7 for the energy and 10e-5 for other parameters. In momentum and continuity equations, the thermo-physical properties are assumed to be temperature independent and, the flow is three-dimensional and steady-state.

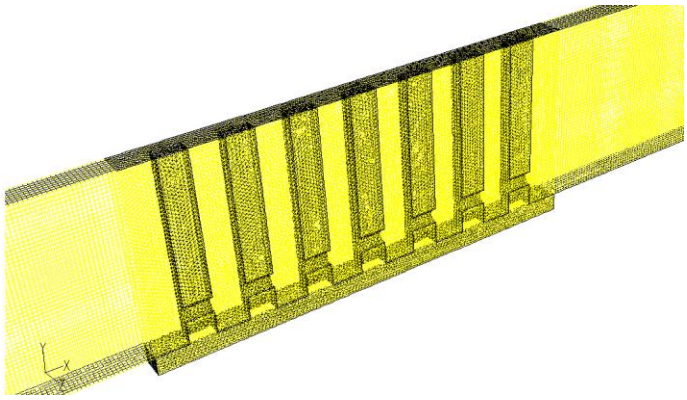

Figure 3. Part of the numerical mesh for the case of C/H=0, S_y/D=1.208.

The part of numerical solution mesh having approximately 802.386 cells is presented in Fig. 3 for the case of C/H=0, S_y/D=1.208. For grid independence, the Nusselt number is used as criterion. The number of volume mesh is varied from 353.206 to 943.882 to obtain the most appropriate mesh number. When the number of the volume mesh reaches to 694.483, no remarkable change in the Nusselt number (less than %3) is observed.

3. HEAT TRANSFER AND FRICTION FACTOR

The Nusselt number is calculated as below:

$$Nu = \frac{h_{av} D_h}{k} \qquad (13)$$

where h_{av} is the average convective heat transfer coefficient, D_h is the hydraulic diameter, and k is the thermal conductivity. The average convective heat transfer coefficient is obtained as:

$$h_{av} = \frac{1}{A_c} \int_0^{A_s} h(A_s) dA_s \qquad (14)$$

Proc. of the Intl. Conf. on Advances In Civil, Structural And Mechanical Engineering- CSM 2014.

ISBN: 978-1-63248-012-5 doi: 10.15224/ 978-1-63248-012-5-79

Here, h is the local convective heat transfer coefficient and is defined as:

$$h = \frac{q''}{T_w(x) - T_m(x)} \qquad (15)$$

Where, q'' is the heat flux, T_w and T_m are the local wall and mean temperatures, respectively.The Reynolds number and friction factor are defined by using Eqs. 16 and 17,

$$\mathrm{Re} = \frac{u_m D_h}{\nu} \qquad (16)$$

$$f = \frac{\Delta P}{\frac{1}{2}\rho u_m^2 \frac{L_t}{D_h}} \qquad (17)$$

where L_t is the length of the test section. In all calculations, the values of the thermo-physical properties of air were obtained at the bulk mean temperature, in which $T_m = (T_{in} + T_{out})/2$.

4. RESULTS AND DISCUSSION

In numerical studies, the validation of the data obtained is one of the most important and required procedure. In this study, the numerical method used is validated via the results obtained for smooth channel with respect to Nusselt number by Şara [22] and Bilen et al. [2]. Likewise, the validation with respect to the friction factor is made by the well-known correlations proposed by Petukhov [23] and Blasius for smooth channel. The correlations of the Nusselt number proposed by Şara [22] and Bilen [2] given below.

$$Nu = 0.0919\,\mathrm{Re}^{0.706}\,\mathrm{Pr}^{1/3} \qquad (18)$$

$$Nu = 0.13656\,\mathrm{Re}^{0.64} \qquad (19)$$

The friction factor correlations for smooth channel of Petukhov [23] and Blasius are

$$f = (0.790\ln \mathrm{Re} - 1.64)^{-2} \quad 10^4 < \mathrm{Re} < 10^6 \qquad (20)$$

$$f = 0.316\,\mathrm{Re}^{-0.25} \qquad (21)$$

In Figs. 4a and 4b, the variations of both Nusselt number and friction factor for smooth channel with Reynolds number are presented. As seen from these figures, the results of the numerical method used and the correlations are in a good agreement. By the aid of these results, it can be concluded that the numerical method and the solution procedure is accurate.

In Figure 5, the temperature contours are presented in a way that the effects of the change of the pin-fin spacing ratio and the Reynolds number on the temperature gradients can be seen at constant clearance ratio. In the front view of the contours, the temperature distributions are presented in the plane of z=0.015 m. In the top view of the contours, the temperature distributions are presented in the plane of y=0.017 m which corresponds to the center of the perforations).

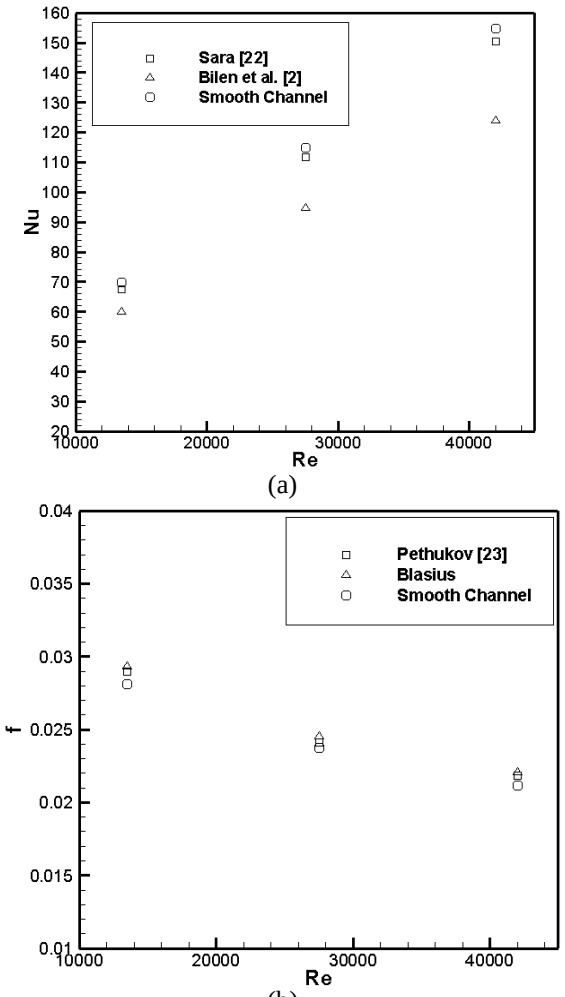

Figure 4. The verification of **(a)** Nusselt number, **(b)** friction factor for smooth channel.

As shown in Figure 5a and b, the surface temperature increases with the increase of the pin-fin spacing ratio. If the pin-fin spacing ratio and the clearance ratio are kept constant (Fig. 6e and f), the temperature of the base plate decreases with increasing Reynolds number. When all these conclusions are evaluated together, it can be concluded that the highest fin (H=100 mm), the smallest pin-fin spacing ratio (S_y/D=1.208) and the biggest Reynolds number (Re=42.000) are found to be better for cooling processes. The temperature distribution on the perforated pin-fins changes in streamwise direction. The temperature of the fins tends to increase towards the end of the test section. In Figure 6, the velocity contours are presented for different cases at z=0.015 m and y=0.017 m. For the case of C/H=0, the velocity of the fluid is fairly high because of the jet flow caused by the cross section narrowing and thus, the highest velocity value inside the perforations is obtained at Re=42.000.

Proc. of the Intl. Conf. on Advances In Civil, Structural And Mechanical Engineering- CSM 2014.

ISBN: 978-1-63248-012-5 doi: 10.15224/ 978-1-63248-012-5-79

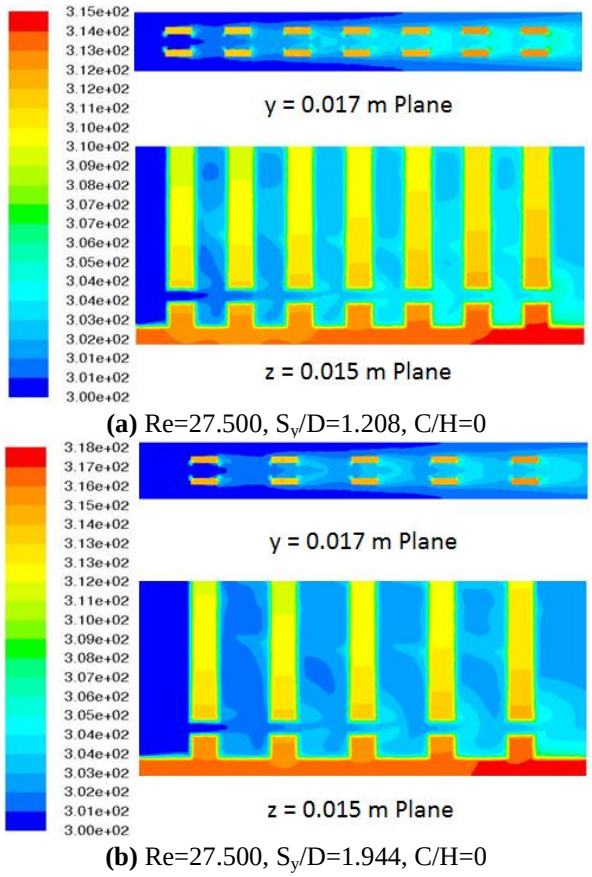

(a) Re=27.500, S_y/D=1.208, C/H=0

(b) Re=27.500, S_y/D=1.944, C/H=0

Figure 5. Temperature contours at different planes and arrangements.

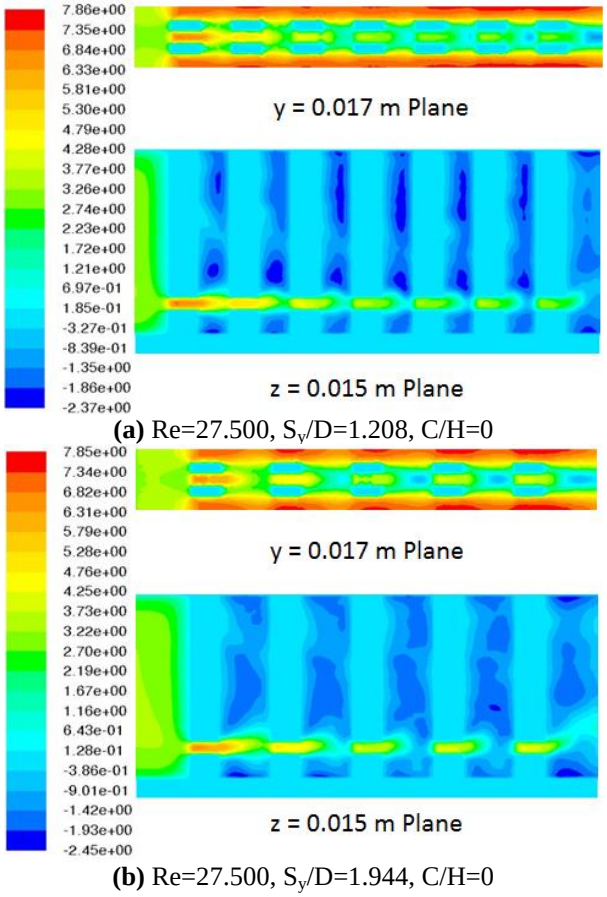

(a) Re=27.500, S_y/D=1.208, C/H=0

(b) Re=27.500, S_y/D=1.944, C/H=0

Figure 6. Velocity contours at different planes and arrangements.

The effects of the perforations opened to create jet flow between the fins are lost remarkably because the flow is blocked in the front side of the fins and, the fluid leave the channel through the by-pass line above the fins. The variations of the Nusselt number with the Reynolds number are shown in Figure 7. As expected, the Nu number increases with increasing Reynolds number while the pin-fin spacing ratio and the clearance ratio are kept constant. As mentioned earlier, adding perforated pin fins into the flow field increases the Nusselt number from seven times to ten times with respect to the smooth channel depending on the arrangement. The highest Nusselt number is obtained as 2449 while the clearance ratio is zero and the pin-fin spacing ratio is 1.208. From the variations of the Nusselt number, it can be concluded that the pin-fin spacing ratio is more effective than the clearance ratio. Extended surfaces (fins) are used to enhance heat transfer. But, the friction factor increases by the use of the fins. Figure 8 shows the variations of the friction factor versus the Reynolds number. The use of the fins in the flow field causes the friction factor to increase. The value of the friction factor increases from 35 times up to 55 times depending on the arrangement type with respect to the smooth channel. The friction factor decreases with increasing Reynolds number. The highest friction factor value is found at S_y/D=1.208 while the clearance ratio is zero because an increase in the number

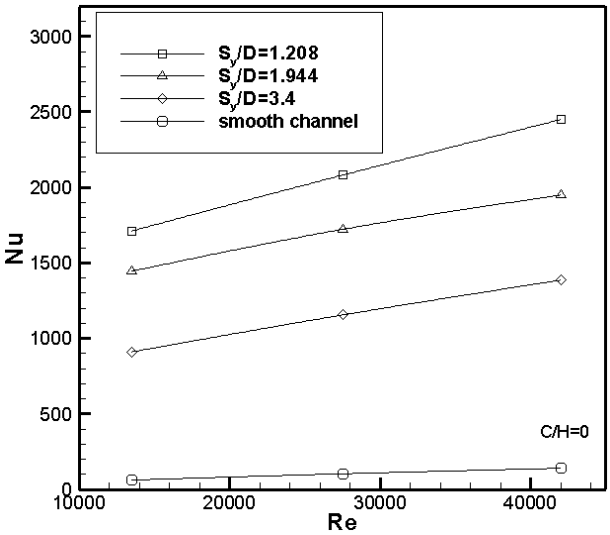

Figure 7. The variation of the Nusselt number versus the Reynolds number.

of the perforated pin-fins and a decrease in the clearance ratio cause more disturbance and friction. In the light of the pressure drop, keeping the clearance ratio constant is a more effective way than enhancing the pin-fin spacing ratio.

Proc. of the Intl. Conf. on Advances In Civil, Structural And Mechanical Engineering- CSM 2014.

ISBN: 978-1-63248-012-5 doi: 10.15224/ 978-1-63248-012-5-79

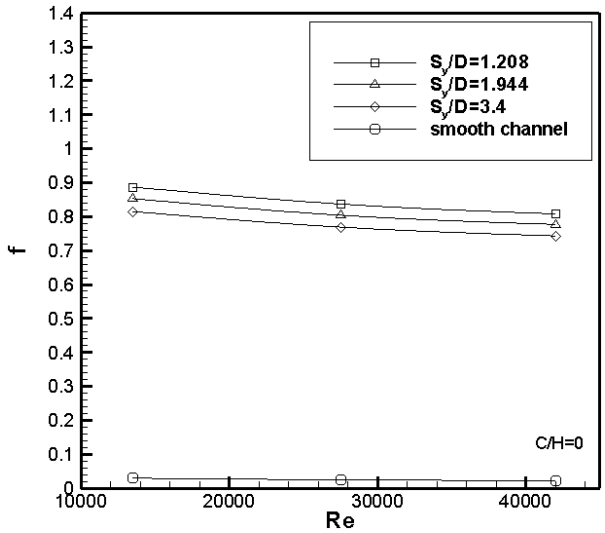

Figure 8. The variation of friction factor versus the Reynolds number.

In heat transfer studies, it is important to evaluate the effects of both the heat transfer and the pressure drop. Therefore, the overall enhancement of each arrangement is presented in Figure 9 versus the Reynolds number to determine the overall gain. If the overall heat transfer enhancement is bigger than one, it is said that there is a net energy gain and, this case is useful with respect to both the heat transfer and the pressure drop.

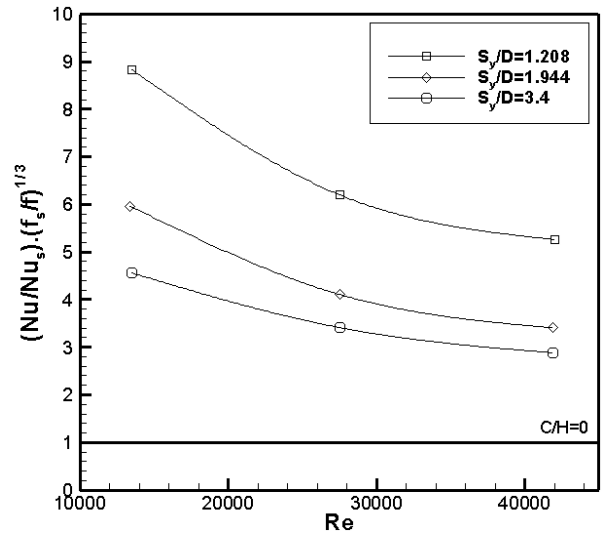

Figure 9. The overal heat transfer enhancement versus the Reynolds number.

5. CONCLUSIONS

Heat transfer and pressure drop characteristics of the perforated pin-fins were numerically determined for different flow velocities, clearance ratios and pin-fin spacing ratios. The results indicated that:

- The The lowest pin-fin spacing ratio of S_y/D=1.208 and the clearance ratio of C/H=0 was better for cooling purposes.
- Adding perforated pin fins into the flow field enhanced the Nusselt number from seven times to ten times with respect to the smooth channel depending on the arrangement. The highest Nusselt number was obtained as 2449 while the clearance ratio was zero and, the pin-fin spacing ratio was 1.208.
- The friction factor decreased with increasing Reynolds number. The highest friction factor value was found at S_y/D=1.208 while the clearance ratio was zero.
- The best overall enhancement was reached at C/H=0, S_y/D=1.208 and Re=13.500. The lowest overall enhancement was obtained for C/H=0, S_y/D=3.4 and Re=42.000.

References

[1] M. Tahat, Z. H. Kodah, B. A. Jarrah and S. D. Probert, Heat transfers from pin-fin arrays experiencing forced convection, *Applied Energy*, vol. 67, pp.419-442, 2000.

[2] K. Bilen, U. Akyol and S. Yapici, Heat Transfer and friction correlations and thermal performance analiysis for a finned surface, *Energy Conversion and Management*, vol. 42, pp. 1071-1083, 2001.

[3] G. Tanda, Heat transfer and pressure drop in a rectangular channel with diamond-sahped elements, *International Journal of Heat and Mass Transfer*, vol. 44, pp. 3529-3541, 2001.

[4] T. M. Jeng, Thermal performance of in-line diamond-shaped pin fins in a rectangular duct, *International Communications in Heat and Mass Transfer*, vol.33, pp. 1139–1146, 2006.

[5] X. L. Yu, Q. K. Feng, Q. P. Liu, Research on the heat transfer and flow performance of a composite heat sink, J Xi'an Jiaotong Univ, Chinese, vol. 37, no.4, pp. 670–3, 2003.

[6] X. L. Yu, Q. K. Feng, J. M. Feng, Research on thermal performance of plate-pin fin heat sink. J Xi'an Jiaotong Univ., Chinese, vol. 38, no. 11, pp. 1114–8, 2004.

[7] X. L. Yu, Q. K. Feng, J. M. Feng, Q.W. Wang, Development of a plate-pin fin heat sink and its performance comparisons with a plate fin heat sink, *Applied Thermal Engineering*, vol. 25, pp. 173–82, 2005.

ISBN: 978-1-63248-012-5 doi: 10.15224/ 978-1-63248-012-5-79

[8] O.A. Leon, G. D. Mey, E. Dick, J. Vierendeels, Staggered heat sinks with aerodynamic cooling fins, *Microelectron Reliability*, vol. 44, pp. 1181–7, 2004.

[9] H. Peng and X. Ling, Analysis of heat transfer and flow characteristics over serrated fins with different flow directions, *Energy Conversion and Management*, vol. 52, pp. 826–835, 2011.

[10] M. H. Şahin, A. R. Dal and E. Baysal, 3-D Numerical study on the correlation between variable inclined fin angles and thermal behavior in plate fin-tube heat exchanger, *Applied Thermal Engineering*, vol. 27, pp. 1806–1816, 2007.

[11] G. Xie and B. Sunden, Numerical predictions of augmented heat transfer of an internal blade tip-wall by hemispherical dimples, *International Journal of Heat and Mass Transfer*, vol. 53, pp. 5639–5650, 2010.

[12] N. Sahiti, A. Lemouedda, D. Stojkovic, F. Durst, E. Franz, Performance comparison of pin fin in-duct flow arrays with various pin cross-sections *Applied Thermal Engineering*, vol. 26, pp. 1176–1192, 2006.

[13] Q. Li, Zh. Chen, U. Flechtner, H. J. Warnecke, Heat transfer and pressure drop characteristics in rectangular channels with elliptic pin fins, *International Journal of Heat and Fluid Flow*, vol. 19, pp. 245–250, 1998.

[14] A. K. Saha and S. Acharya, Parametric study of unsteady flow and heat transfer in a pin fin heat exchanger, *International Journal of Heat Mass Transfer*, vol. 46, pp. 3815–30, 2003.

[15] J. J. Hwang and C. C. Lui, Detailed heat transfer characteristic comparison in straight and 90-deg turned trapezoidal ducts with pin-fin arrays, *International Journal of Heat Mass Transfer*, vol. 42, pp. 4005–16, 1999.

[16] J. J. Hwang and C. C. Lui, Measurement of end wall heat transfer and pressure drop in a pin-fin wedge duct, *International Journal of Heat Mass Transfer*, vol. 45, pp. 877–89, 2002.

[17] B. Sahin and A. Demir, Performance analysis of a heat exchanger having perforated square fins, *Applied Thermal Engineering*, vol. 28, pp. 621–632, 2008.

[18] B. Sahin and A. Demir, Thermal performance analysis and optimum design parameters of heat exchanger having perforated pin fins, *Energy Conversion and Management*, vol. 49, pp. 1684-1695, 2008.

[19] O.N. Sara, T. Pekdemir, S. Yapici, M. Yılmaz, Heat-transfer enhancement in a channel flow with perforated rectangular blocks, *International Journal of Heat and Fluid Flow*, vol. 22, pp. 509–518, 2001.

[20] P. Naphon and A. Sookkasem, Investigation on heat transfer characteristics of tapered cylinder pin fin heat sinks, *Energy Conversion and Management*, vol. 48, pp. 2671–2679, 2007.

[21] FLUENT 6.1.22., User's Guide, Fluent Incorporated, Centerra Resource Park, 10 Cavendish Court, Lebanon, NH 03766, USA, 2001.

[22] O. N. Sara, Performance analysis of rectangular ducts with staggered square pin fins, *Energy Conversion and Management*, vol. 44, pp. 1787-1803, 2003.

[23] B. S. Pethukov, Heat transfer in turbulent pipe flow with variable physical properties. In: Harnett JP, editor. Advances in heat transfer, vol. 6. New York: Academic Press; p. 504–64, 1970.